

The Formation of High Redshift Submillimeter Galaxies

Desika Narayanan^{1*†}, Christopher C. Hayward¹, Thomas J. Cox^{1‡}, Lars Hernquist¹, Patrik Jonsson², Joshua D. Younger^{1,4§}, and Brent Groves³

¹Harvard-Smithsonian Center for Astrophysics, 60 Garden St., Cambridge, Ma 02138

²Santa Cruz Institute for Particle Physics, University of California, Santa Cruz, Santa Cruz, Ca

³Sterrewacht Leiden, Neils Bohrweg 2, Leiden 2333-CA, The Netherlands

⁴Current Address: Institute for Advanced Studies, Einstein Drive, Princeton, NJ 08544

Accepted by MNRAS

ABSTRACT

We describe a model for the formation of $z \sim 2$ Submillimeter Galaxies (SMGs) which simultaneously accounts for both average and bright SMGs while providing a reasonable match to their mean observed spectral energy distributions (SEDs). By coupling hydrodynamic simulations of galaxy mergers with the high resolution 3D polychromatic radiative transfer code SUNRISE, we find that a mass sequence of merger models which use observational constraints as physical input naturally yield objects which exhibit black hole, bulge, and H_2 gas masses similar to those observed in SMGs. The dominant drivers behind the 850 μm flux are the masses of the merging galaxies and the stellar birthcloud covering fraction. The most luminous ($S_{850} \gtrsim 15$ mJy) sources are recovered by $\sim 10^{13} M_{\odot}$ 1:1 major mergers with a birthcloud covering fraction close to unity, whereas more average SMGs ($S_{850} \sim 5\text{--}7$ mJy) may be formed in lower mass halos ($\sim 5 \times 10^{12} M_{\odot}$). These models demonstrate the need for high spatial resolution hydrodynamic and radiative transfer simulations in matching both the most luminous sources as well as the full SEDs of SMGs. While these models suggest a natural formation mechanism for SMGs, they do not attempt to match cosmological statistics of galaxy populations; future efforts along this line will help ascertain the robustness of these models.

Key words: cosmology:theory–galaxies:formation–galaxies:high-redshift–galaxies:interactions–galaxies:ISM–galaxies:starburst

1 INTRODUCTION

As a population, $z \sim 2$ Submillimeter Galaxies (SMGs) are the most luminous, heavily star-forming galaxies in the Universe (Blain et al. 2002). The last decade of observations have provided significant constraints regarding their physical properties. Selected for their prodigious long wavelength emission ($\gtrsim 5$ mJy at 850 μm), SMGs are thought to be starburst dominated (Chapman et al. 2004; Alexander et al. 2008; Younger et al. 2008a), and have massive $\sim 10^{10}\text{--}10^{11} M_{\odot}$ H_2 gas reservoirs (Tacconi et al. 2006, 2008; Greve et al. 2005). If stars form according to a Kroupa initial mass function (IMF), as is supported by observations (Tacconi et al. 2008), then the infrared luminosities from SMGs translates to tremendous inferred $\sim 700\text{--}1500 M_{\odot} \text{yr}^{-1}$ star formation rates (Kovács et al. 2006; Pope et al. 2008) driven by major mergers (Tacconi et al. 2008). SMGs are extremely massive, with typical

$\sim 5 \times 10^{11} M_{\odot}$ bulges in place (Borys et al. 2005; Swinbank et al. 2004), and are a highly clustered population of galaxies, residing in $\sim 10^{12}\text{--}10^{13} M_{\odot}$ dark matter halos (Blain et al. 2004; Swinbank et al. 2008).

Understanding SMGs from a theoretical standpoint has proven a major challenge for models. Recently, by assuming a flat stellar initial mass function (IMF) for starbursting galaxies (such that $d n / d(\ln m) = m^{-x}$ with $x = 0$ as compared to 1.35 for Salpeter’s IMF)¹, semi-analytic models (SAMs) of galaxy formation coupled with 2-D spectrophotometric simulations (Silva et al. 1998) have successfully reproduced the observed SMG number counts at $z \sim 2$. Though these models have struggled to match some details of SMGs (e.g. the K -band through mid-IR SEDs; Swinbank et al. 2008), it is clear from these models that, in principle, SMGs

* E-mail: dnarayanan@cfa.harvard.edu

† CfA Fellow

‡ W.M. Keck Postdoctoral Fellow

§ Hubble Fellow

¹ Though the issue of the IMF in $z \sim 2$ SMGs is controversial (Baugh et al. 2005; Swinbank et al. 2008; Tacconi et al. 2008; Davé 2008; van Dokkum 2008), we do not attempt to investigate the role of the IMF in reproducing cosmological number counts in this paper; this will be investigated in due course.

broadly fit into our current understanding of high- z galaxy formation.

However, while the SAMs provide insight into the cosmological properties of SMGs, their usage of simplified analytic prescriptions for star formation and AGN activity mean that detailed information on the formation, evolution, and physical properties of individual SMGs is lacking. In this arena, high resolution hydrodynamic simulations are better suited, yet thus far have struggled. While recent theoretical work utilizing gas rich galaxy merger simulations has shown good success in reproducing the observed characteristics of a number of galaxy populations – e.g. quasars (Hopkins et al. 2005, 2006a, and references therein), red galaxies (Springel et al. 2005a; Hopkins et al. 2006b, 2008b), elliptical galaxies (Cox et al. 2006; Hopkins et al. 2008a,c, 2009a,b), and warm Ultraluminous Infrared Galaxies (Younger et al. 2009a) – a detailed model for SMG formation and evolution using simulations has remained elusive. For example, attempts at forming SMGs by combining hydrodynamic and radiative transfer calculations of gas rich mergers have shown a peak flux of only $\sim 4\text{--}5$ mJy in the submillimeter for the most massive ($M_{\text{DM}} \approx 2 \times 10^{13}$) and luminous sources (Chakrabarti et al. 2008). This is only marginally detectable in current deep, wide cosmological surveys (Coppin et al. 2006), and has dark matter and stellar masses too large to be representative of the average SMG population (Alexander et al. 2008; Swinbank et al. 2008).

This Letter is the first in a series of papers attempting to understand the detailed properties of SMGs using simulations. Here, we present the first model for the formation of SMGs that reproduces both average and bright SMGs while plausibly matching their mean observed SEDs, and stellar bulge, H_2 , and black hole masses. We show that high resolution hydrodynamic and radiative transfer simulations are necessary to capture both the requisite starbursts as well as stellar bulge growth and dust obscuration to simultaneously power both the most luminous SMGs and match the observed SEDs. Throughout this paper, we assume $\Omega_{\Lambda} = 0.7$, $\Omega_M = 0.3$, and $h = 0.7$.

2 NUMERICAL METHODS

We follow the hydrodynamic evolution of galaxy mergers of varying mass and mass ratios using the N -body plus smoothed particle hydrodynamics (SPH) code GADGET3 (Springel 2005). The synthetic photometric properties of the simulations are then calculated using the 3D adaptive mesh Monte Carlo polychromatic radiative transfer code, SUNRISE (Jonsson 2006). Our goal throughout is to utilize physical parameter input to the models directly constrained by observations of SMGs where possible, and from local ULIRGs or the Milky Way Galaxy when data from SMGs may not be available.

2.1 Hydrodynamics

GADGET3 utilizes an entropy-conserving formalism for SPH (Springel & Hernquist 2002) which include prescriptions for radiative cooling of the gas (Katz et al. 1996; Davé et al. 1999), and a sub-grid formalism for a multi-phase interstellar medium (ISM) in which cold clouds are embedded in a hot, pressure confining phase (Springel & Hernquist 2003). The cold clouds are allowed to grow through radiative cooling of the hot phase gas, and similarly, supernovae may evaporate the cold gas into the hotter phase. Numerically, supernovae pressurization of the ISM is handled through

an effective equation of state (EOS). Here, we employ a stiff EOS with $q_{\text{EOS}} = 1$ (see Fig 4. of Springel et al. 2005b) which allows for stable disk evolution. Star formation in the simulations proceeds following a generalized Kennicutt-Schmidt (KS) relation (e.g. $\text{SFR} \propto \rho^{1.5}$) with normalization set to match the local surface density relation. This assumption is bolstered by observations of SMGs which hint at a KS index near the locally observed value, 1.5 (Bouché et al. 2007).

Black holes are included in the simulations as sink particles that accrete surrounding material following an Eddington limited Bondi-Hoyle-Lyttleton parameterization (e.g. Bondi & Hoyle 1944). A subresolution model for feedback is incorporated as an isotropic thermal coupling between the active galactic nucleus (AGN) and the surrounding ISM. The efficiency of this coupling is tuned to match the local M - σ relation (Di Matteo et al. 2005).

The galaxies are initialized with a Hernquist (1990) dark matter profile, and virial properties scaled to be appropriate for redshift $z \sim 3$ (Robertson et al. 2006). The galaxies are initialized with circular velocities $V_{\text{circ}} = 320 - 500 \text{ km s}^{-1}$, motivated by the circular velocities for SMGs measured by Tacconi et al. (2008). This results in halo masses of $M_{\text{DM}} \sim 10^{12} - 10^{13} M_{\odot}$, consistent with SMG clustering measurements (Blain et al. 2004). The galaxies are bulgeless, and the initial gas fraction is 80%. This results in galaxies with gas fractions $\lesssim 40\%$ at final coalescence (owing to gas consumption by star formation), comparable to estimates of observed SMGs (Bouché et al. 2007). Our gas particle masses were $M = 1.4 \times 10^6 h^{-1} M_{\odot}$, and softening lengths $100 h^{-1} \text{ pc}$. In this paper, we consider 12 merger models varying mass, merger orbit and mass ratio. We consider 1:1 mergers in $\sim 10^{12}$, 5×10^{12} and $10^{13} M_{\odot}$ halos, and 1:3 and 1:12 mergers with a $M_{\text{DM}} \approx 10^{13} M_{\odot}$ primary galaxy.

2.2 Radiative Transfer

SUNRISE considers the propagation of radiation between UV and millimeter wavelengths through a dusty medium (see Jonsson (2006) for greater detail, as well as Jonsson et al. (2009) for important updates, some of which are summarized here). SUNRISE tracks model photon ‘packets’ originated by sources – AGN, stellar clusters, and the ISM itself – as they traverse the dusty ISM using a Monte Carlo methodology. As in galaxies in nature, the flux emergent from the model galaxy/galaxies is determined by the photons that are emitted from the stars or AGN in the camera direction and escape without interacting and also the photons that scatter or are re-emitted by dust into the camera direction. Here, we utilized 8 different cameras distributed uniformly around the model galaxy/galaxies. SUNRISE treats dust self-absorption and re-emission in calculating the dust temperature.

New for the simulations here, the AGN emits an empirical template SED derived from observations of unobscured quasars (Hopkins et al. 2007), assuming a radiative efficiency of 10%. The normalization of this input spectrum is set by the total bolometric luminosity of the central black hole. The spectrum emitted from stellar clusters is calculated utilizing *Starburst 99* (Leitherer et al. 1999). We assume a Kroupa IMF for the stars, which is in good agreement with the estimates for $z \sim 2$ galaxies (Davé 2008; Tacconi et al. 2008; van Dokkum 2008). For young stellar clusters, which are still located in their nascent birthclouds of molecular gas, the input spectrum includes the effects of the HII regions and photodissociation regions (PDRs) surrounding the clusters (Groves et al. 2008). The models describe the evolution of the HII regions and PDRs analytically and use the photoionization

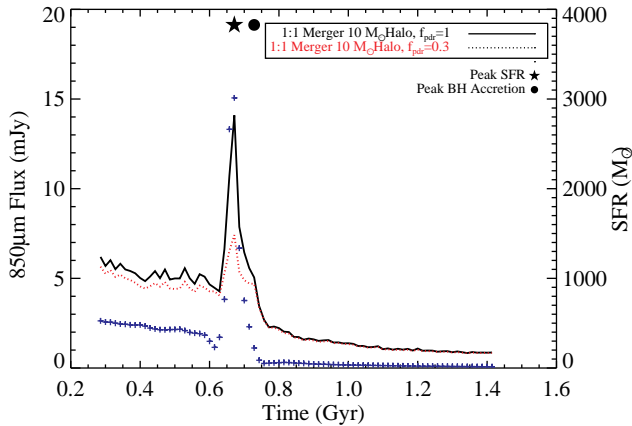


Figure 1. Evolution of 850 μm flux from model 1:1 major merger in a $\sim 10^{13} M_{\odot}$ halo. Two different birthcloud covering fractions (f_{pdr}) are shown (black solid line and red dashed line). The blue crosses represent the SFR with units on the right axis. The black star and dot near the top axis denote the peak of the starburst and black hole accretion rate, respectively. During the peak starburst, the opacity is dominated by stellar birthclouds, and the galaxy may be seen as an SMG. The most massive mergers with birthcloud covering fractions of unity may represent the most luminous observed SMGs.

code MAPPINGSIII (Groves et al. 2004) to calculate the SED that emerges from the cluster after it has been reprocessed by the HII regions and PDRs. The HII region absorbs almost all of the ionizing radiation and is responsible for the hydrogen emission lines and hot dust emission. The PDR absorbs a significant fraction of the UV stellar light and reprocesses it to FIR emission via cooler dust.

A fraction (f_{PDR}) of clusters with ages < 10 Myr are modeled as obscured by their nascent birth clouds. As this fraction is increased, more UV and optical flux is reprocessed to longer wavelengths. The covering fraction affects the maximum sub-mm luminosity during the peak of the starburst. This is equivalent to a cloud clearing time scale. While $f_{\text{pdr}} \approx 0.2$ (which corresponds to a clearing timescale ~ 2 Myr) may be a reasonable approximation for field galaxies (Groves et al. 2008), in the case of massive, gas rich galaxy mergers, an assumption of $f_{\text{PDR}} \approx 1$ ($t_{\text{clear}} \gg 10$ Myr) may be more appropriate. Indeed, observations of molecular gas in local ULIRGs have found that the nuclear regions of mergers are often best characterized by a uniform molecular medium, rather than discrete clouds (Downes & Solomon 1998; Sakamoto et al. 1999). While this is not the same as a birthcloud covering fraction of unity, tests done for this work have shown that they result in similar FIR/submm fluxes². We note that the simulations do not account for the obscuration of stellar light by GMCs outside of the birthcloud.

We utilize 10^7 photon packets per iteration in the radiative equilibrium calculations, and the analysis is done for rest frame wavelengths 0.1 to 1000 μm . The stellar particles initialized with the simulation are assumed to have formed at a constant rate over ~ 250 Myr. Metal enrichment is tracked from supernovae using an

² We have run experiments assuming $f_{\text{pdr}} = 0$, and that each grid cell is uniformly filled with dust with mass set by the ULIRG dust to gas ratio. In this limiting case, we find fluxes quite similar to those in simulations where the PDR covering fraction is unity.

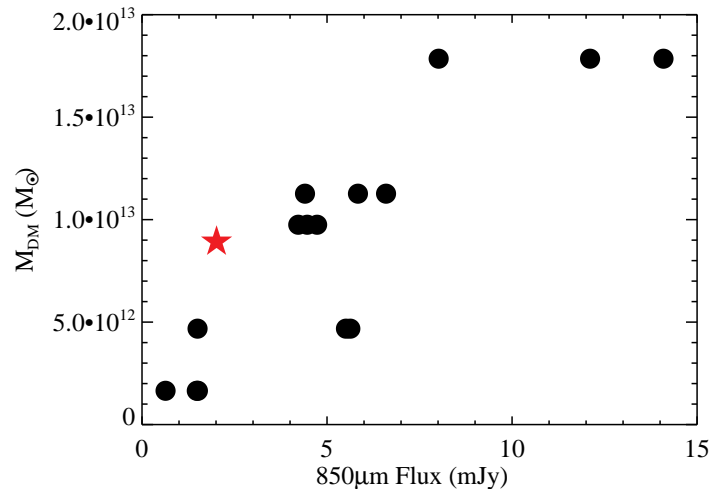


Figure 2. Total halo mass versus peak S_{850} . The full range of observed 850 μm fluxes from SMGs may be understood from a mass sequence merger models, varying only total mass. More massive mergers induce stronger bursts which fuel more luminous SMGs. The red star shows an isolated disk. Some merging activity may be necessary to induce the necessary SFRs to form SMGs. Even massive ($\sim 10^{13} M_{\odot}$) isolated disks seem unable to reach the nominal $S_{850} > 5$ mJy detection threshold, though may be routinely detectable via future-generation bolometers.

instantaneous recycling approximation. The gas and stars initialized with the simulation are assigned a metallicity according to a closed-box model such that $Z = (-y \ln[f_{\text{gas}}])$ where Z is the metallicity, y the yield=0.02, and f_{gas} is the initial gas fraction (though note the fluxes during the SMG phase of the model galaxies is not very sensitive to these assumptions). Without knowledge of the dust properties of $z \sim 2$ SMGs, we conservatively assume a 3.1₆₀ Draine & Li (2007) model. We additionally assume a constant dust to gas ratio comparable to that of ULIRGs (1/50; Wilson et al. 2008) which tentative evidence suggests is appropriate for SMGs (Kovács et al. 2006; Greve et al. 2005; Tacconi et al. 2006). We have additionally run models assuming a Milky Way dust to metals ratio of 0.4 (Dwek 1998), and found similar results to within 10%. We note that comparisons to templates which include stochastically heated grains (Draine & Li 2007) suggest a potential uncertainty in the FIR SED up to a factor of 2 (Jonsson et al. 2009).

3 RESULTS

3.1 Formation of a Submillimeter Galaxy

Galaxy mergers residing in halos with masses comparable to those observed naturally produce submillimeter galaxies with a range of 850 μm fluxes during their peak starburst phase. Mergers with a total halo mass above $\sim 5 \times 10^{12} M_{\odot}$ will produce galaxies above the nominal SMG detection threshold ($S_{850} \gtrsim 5$ mJy) whereas significantly lower mass mergers may not. The peak observed submillimeter flux is dependent on the total dust obscuration for a given merger model.

To see this, in Figure 1, we begin by showing the evolution of the 850 μm flux (at $z = 2$, the rough mean redshift for radio-selected SMGs; Chapman et al. 2003b) for a $M_{\text{DM}} \approx 10^{13} M_{\odot}$ 1:1 merger for two birthcloud covering fractions. Additionally, we overplot the

Table 1.

Total M_{DM} M_{\odot}	Mass Ratio	M_{\star} M_{\odot}	M_{H_2} M_{\odot}	M_{BH}^a M_{\odot}	Peak S_{850} mJy
2×10^{13}	1:1	8×10^{11}	1.5×10^{11}	3.3×10^8	14.1
1.1×10^{13}	1:3	2.8×10^{11}	3×10^{10}	*	6.6
7×10^{12}	1:1	2×10^{11}	1.8×10^{10}	0.8×10^8	5.6
9.8×10^{12}	1:12	2.9×10^{11}	2×10^{10}	*	4.8

^a Owing to long dynamical friction time scales, minor mergers tend to be relatively gas poor upon final coalescence, and show their largest burst of 850 μm flux on first passage. While BH growth is generally self-regulated, and the final coalescence BH masses are robust for a large range of initial BH seed masses, M_{BH} for first passage starbursts can vary wildly based on initial seed masses (Younger et al. 2008b). As such, the BH masses for first-passage SMGs in the simulations are relatively uncertain.

SFR in light blue symbols. During the first passage and in-spiral phase of a galaxy merger, the galaxies are forming stars (individually) at $\sim 100\text{--}200 M_{\odot}\text{yr}^{-1}$. During this time, obscuration by the diffuse ISM dominates and produces a modest ~ 5 mJy of emission seen during the in-spiral phase, regardless of the GMC covering fraction.

As the galaxies reach final coalescence ($T \sim 0.65$ Gyr), tidal torquing of the gas fuels a $\sim 2000 M_{\odot}\text{yr}^{-1}$ nuclear starburst. At this time, the FIR/submillimeter flux is dominated by cold dust re-processing of UV photons in young stellar clusters by their birthclouds. Hence, the submillimeter flux rises rapidly with this burst in star formation rendering the galaxy detectable as an extremely luminous SMG for a relatively short (< 50 Myr) lifetime. The peak flux of the SMG produced in the final burst is dependent on the birthcloud covering fraction. The merger model in Figure 1 with a covering fraction of 30% reaches a peak flux of $\sim 7\text{--}8$ mJy, whereas the model with covering fraction of unity produces an SMG comparable to the most luminous observed sources. The obscuration of young stars is vital to creating the most luminous SMGs as these stars dominate the bolometric luminosity of the galaxy during coalescence.

Because the peak flux received is primarily determined by the strength of the starburst (for a given birthcloud covering fraction), the submillimeter flux is dependent on the mass of the merger. Less massive galaxies will induce smaller tidal torques on the gas, fueling lower SFRs; in these cases, the lightcurve shown for the massive merger in Figure 1 will retain its shape, though simply lower in normalization. In Figure 2, we indicate this more explicitly by showing the predicted 850 μm flux against the galaxy (halo) mass of all 12 merger models varying primary halo mass, mass ratio (1:1, 1:3 and 1:12) and orbit. Again, the 850 μm flux is modeled at $z = 2$. A single isolated disk is shown by the red star. Each is assumed to have a constant birthcloud covering fraction of unity.

The 1:1 major mergers in the most massive ($M_{\text{DM}} \approx 2 \times 10^{13} M_{\odot}$) halos produce SMGs comparable to the most luminous observed (Coppin et al. 2006; Pope et al. 2006). Galaxies $\sim 2\text{--}4$ times smaller may be representative of more average ($S_{850} \sim 5$ mJy) SMGs. Galaxies well below this mass limit are unlikely to ever produce SMGs based on the current fiducial criteria $S_{850} \gtrsim 5$ mJy, though may be detectable with sensitive new bolometer arrays. As is shown by the isolated galaxy (red star, Figure 2), some merging seems to be necessary to fuel the starbursts that power SMGs. Isolated galaxies residing in even the most massive halos

in our simulations ($M_{\text{DM}} \approx 10^{13} M_{\odot}$) never appear to get above $\sim 2\text{--}3$ mJy at 850 μm .

3.2 Physical Properties and SEDs of SMGs

The SMGs produced by the galaxy mergers presented here have black hole, stellar, H_2 , and dark matter masses (the latter by construction) comparable to those observed. In Table 3, we show these values for a typical orbit ($\theta_1, \phi_1 = (30, 60)^\circ$, $\theta_2, \phi_2 = (-30, 45)^\circ$) for the simulations which produced detectable SMGs. As shown in Cox et al. (2009, submitted) and Narayanan et al. (2008), binary galaxy mergers produce $\sim 90\%$ of their final stellar mass during the pre-coalescence phase. As such, the bulk of the $\sim 10^{11} M_{\odot}$ bulges are already in place during when the galaxy is visible as an SMG. Indeed, this is clear from a visual integration of the SFR in Figure 1; an SFR of a few $\times 10^2 M_{\odot}\text{yr}^{-1}$ for $\sim 5 \times 10^8$ years results in a few $\times 10^{11} M_{\odot}$ bulge.

The black hole growth follows a different story: the bulk of the growth occurs concomitant to the SMG phase/final coalescence. While the final black hole masses in the most massive/luminous systems may be similar to those of $z \sim 2$ quasars ($\sim 10^9 M_{\odot}$), during the SMG phase they can be a factor of $\sim 3\text{--}10$ lower than these final values. This gives them masses of order $\sim 10^8 M_{\odot}$, comparable to observed values (Alexander et al. 2008, and references therein). Finally, as was noted in § 2, by starting with progenitor galaxies with gas fractions $f_g = 0.8$, the final gas fraction of during the SMG phase is $\lesssim 40\%$, comparable to estimates of observed SMGs (Bouché et al. 2007). While GADGET3 does not track the evolution of molecular gas, we derive the molecular gas fraction in post-processing based on the ambient pressure on the cold, star-forming ISM (see Blitz & Rosolowsky 2006). From this, we find total H_2 gas masses between $10^{10} - 10^{11} M_{\odot}$ (Table 3). This is comparable to measurements by Greve et al. (2005) and Tacconi et al. (2006). Moreover, complementary radiative transfer simulations by Narayanan et al. (2009) utilizing this methodology for assigning the H_2 gas fraction have shown good correspondence between the simulated CO properties (e.g. excitations and line widths) of these model SMGs, and those in nature.

Galaxy mergers in a mass range of $M_{\text{DM}} \approx 5 \times 10^{12} M_{\odot} - 10^{13} M_{\odot}$ naturally produce SMGs with optical through mm-wave SEDs comparable to those observed. In Figure 3, we show the model SED for all snapshots in the merger simulations studied here which produce an SMG with $S_{850} > 5$ mJy, redshifted to $z = 2$. The blue shaded region shows the 1σ dispersion amongst all snapshots

which satisfy this fiducial selection criterion while the black solid line shows the mean amongst snapshots. The mean observed data points from the surveys of Chapman et al. (2005, purple triangles), Hainline et al. (2009, red crosses), and Kovács et al. (2006, green diamonds) are overlaid. Only observational data with spectroscopic redshifts are utilized.

The SED encodes information regarding the young stars (at $z \sim 2$, observed-frame K -band), stellar mass (observed mid-IR), and cold dust obscuration levels (observed submillimeter). The SFR and stellar bulge growth are explicitly tracked in the progenitor galaxies and SMG by the high resolution SPH simulations while the dust obscuration is modeled globally by diffuse dust, and on local scales by the subgrid implementation of the MAPPINGSIII photoionization calculations. Because the SFRs in the simulated galaxies are comparable to those observed, and bulges of order $\sim 1\text{--}8 \times 10^{11} M_{\odot}$ are in place during the SMG phase (see Table 3), the observed K -band and mid-IR fluxes in the model SED match the observed data points closely. Sufficient cold dust obscuration provided by the diffuse dust and birthclouds reprocesses the rest-frame UV emission into the cold dust tail providing a good match to the mean observed 350, 850, and 1100 μm data points. The cases with lower birthcloud covering fraction ($f_{\text{pdr}} = 0.3$) tend to overestimate the rest-frame UV and optical flux by a factor of ~ 2 .

While our simulations do not include radio emission, we can estimate the radio properties of our simulations by assuming that the far-IR/radio correlation does not evolve strongly with redshift (e.g. Kovács et al. 2006; Younger et al. 2009b; Sajina et al. 2008, Younger et al. 2009, in press). We estimate the FIR flux via the standard $\text{FIR} = 1.26 \times 10^{-14} (2.58 S_{60} + S_{100}) \text{ W m}^{-2}$, where S_{60} and S_{100} are the observed-frame fluxes at 60 and 100 μm , in Jy), and then relate the FIR flux to the radio (1.4 GHz) flux through the FIR-radio correlation (e.g. Equation 5 from Kovács et al. 2006). We assume a range of q -parameters, from 2.14 (consistent with observations of SMGs; Kovács et al. 2006), to the locally-observed value for IRAS BGS galaxies, $q = 2.35$ (Sanders & Mirabel 1996). We include bandwidth compression and a K -correction (assuming an SED slope of $\alpha = 0.7$, typical for synchrotron power laws; Condon 1992) when redshifting the radio flux. We note that this method neglects any potential radio contribution from the AGN. When using the observed FIR-radio correlation for SMGs, we recover inferred 1.4 GHz flux densities (at $z = 2.0$) of 20–700 μJy . The average value amongst our simulation sample for a $q=2.14(2.35)$ is $S_{1.4} \approx 125(95) \mu\text{Jy}$, similar to values described in the compilation by Chapman et al. (2003a). The $850/S_{1.4}$ flux density ratios from our simulated SMGs is additionally in good agreement with measurements from recent surveys (e.g. Pope et al. 2006). For example, we find the mean $850/S_{1.4}$ ratio for $S_{850} > 5 \text{ mJy}$ SMGs to be ~ 60 (with a 1σ dispersion of 40) when utilizing $q=2.14$. The mean(dispersion) increases to 100(65) when utilizing the local q .

The SMGs formed in these simulations would generally have a high detection fraction of radio counterparts. In Figure 4, we plot the inferred 1.4 GHz flux density (derived utilizing $q = 2.14$) versus S_{850} at $z=2.0$ for all model galaxies in our simulations. We extend the nominal detection threshold to $S_{850} > 1 \text{ mJy}$ to serve as a prediction. SMGs ($S_{850} > 5 \text{ mJy}$) at $z=2.0$ will typically be detectable down to $\sim 100 \mu\text{Jy}$ at 1.4 GHz. While it is difficult to make quantitative comparisons to observed detection fractions, owing to the fact that these simulations are not cosmological (and S_{850} is roughly constant with increasing redshift while $S_{1.4}$ decreases rapidly with increasing z), it is still feasible to make qualitative comparisons to observations. Observed SMGs have a high

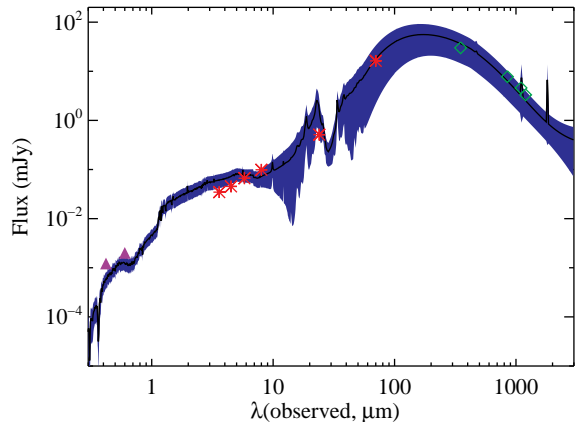


Figure 3. Mean SED of all snapshots from merger simulations satisfying the $S_{850} > 5 \text{ mJy}$ selection criterion for SMGs (solid line). The dispersion amongst the snapshots is shaded in blue (the dispersion amongst viewing angles, however, is not shown). The simulated SED has been redshifted to $z = 2$. Observed data points from Chapman et al. (2005), Hainline et al. (2009, submitted) and Kovács et al. (2006) are overlaid (purple triangles, red crosses and green diamonds, respectively). These data all have spectroscopic redshifts. The points represent the mean observed value from these surveys, though galaxies with $z < 1$ and upper limits have been discarded. The model SED from the fiducial merger provides a good match to the observed photometric data from the B -band to 1 mm, making this the first model SMG to reproduce the full optical through mm-wave SED.

incidence of radio counterparts. Large radio ID fractions were reported by Ivison et al. (2002), who found that nearly all $S_{850} > 10 \text{ mJy}$ SMGs were detected above $\sim 35 \mu\text{Jy}$ at 1.4 GHz, and approximately half the SMGs above $S_{850} > 5 \text{ mJy}$ were radio-detected. More recently, Wagg et al. (2009) find that some $\sim 80\%$ of the SMGs in their sample contain radio counterparts above $\sim 25 \mu\text{Jy}$. More generally, the dynamic range probed by the submillimeter flux densities and radio flux densities in Figure 4 is comparable to that seen in the S_{850} - $S_{1.4}$ relation compiled by Chapman et al. (2003a).

Many of the model SMGs in these simulations have multiple radio counterparts. In Figure 5, we show the optical (SDSS z, r, u) morphologies of our most luminous simulated SMG through its inspiral with a contour denoting the location of the bulk of the radio emission (contours enclose regions where $S_{1.4} > 0.1 \mu\text{Jy}$). As the galaxies in Figure 5 spiral in toward coalescence, they may be visible as multiple radio sources. There is a trend for the more massive/luminous SMGs to have multiple counterparts for a larger fraction of their lives. This owes to the fact that the most massive mergers (e.g. $M_{\text{DM}} > 10^{13} M_{\odot}$) can be SMGs during their inspiral phase (e.g. Figure 1), whereas less massive galaxies (e.g. $M_{\text{DM}} \approx 5 \times 10^{12} M_{\odot}$) generally only reach $S_{850} > 5 \text{ mJy}$ when the progenitor galaxies have coalesced. To identify individual radio sources, we search for the peaks in the radio emission (as inferred from the FIR-radio correlation) in maps which view the galaxies at an arbitrary angle. We then assign the peaks as originating in separate galaxies when they originate at least 5 kpc apart. Utilizing this prescription, we find that the least massive/luminous SMGs in our simulations never have multiple radio counterparts. However, the SMGs formed in $M_{\text{DM}} \approx 1(2) \times 10^{13} M_{\odot}$ halos have multiple radio counterparts $\sim 50(75)\%$ of the time that they would be submillimeter-identified ($S_{850} > 5 \text{ mJy}$).

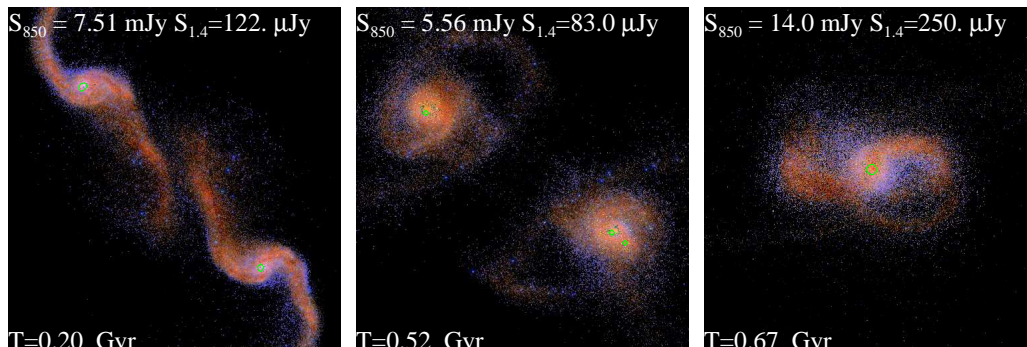


Figure 5. Optical (Sloan z, r, u) colors mapped onto R,G,B for the most massive/luminous SMG in our simulation sample. The thick green contours toward the galactic nuclei of each image enclose the region where the radio emission is above $S_{1.4\text{GHz}} > 0.1 \mu\text{Jy}$. Note, the contours are only at a single level. During the inspiral phase of this massive ($M_{\text{DM}} \approx 2 \times 10^{13} M_{\odot}$) merger, the galaxy may be viewed as having multiple radio counterparts.

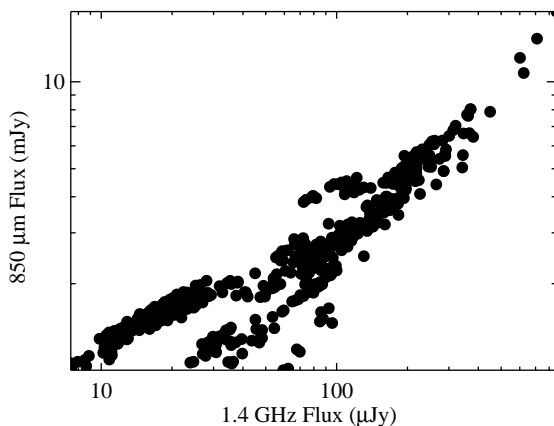


Figure 4. S_{850} versus 1.4 GHz inferred flux density at $z=2.0$ for all models in Table 3. Given current flux limits, the SMGs simulated here will have a high incidence of radio counterparts.

4 DISCUSSION AND CONCLUSION

The models presented here have shown that merger-driven SMG formation simulations which utilize observational parameters as input produce both average ($S_{850} \sim 5$ mJy) and bright ($S_{850} \gtrsim 15$ mJy) SMGs while reproducing observed physical characteristics, as well as the full optical-mm wave SED. This match between simulations and observations is only possible because of the high resolution approach employed for both the hydrodynamic and subgrid physics included in the radiative transfer simulations. It is worth briefly comparing these results to previous efforts in modeling SMG formation to place our models in context.

Models attempting to form SMGs by Chakrabarti et al. (2008) utilized binary galaxy mergers similar to these. The peak submillimeter flux from mergers comparable to the most massive observed ($M_{\text{DM}} \approx 2 \times 10^{13} M_{\odot}$) in this work showed ~ 4 -5 mJy at 850 μm ; this is compared to ~ 15 mJy from comparable mass simulations at an identical merger orbit presented here. While the hydrodynamic evolution of the galaxy mergers is similar in both studies, the radiative transfer differs significantly. In particular, here, we employ a subgrid model for including the obscuration by the nascent birthclouds of young stellar clusters. As Figure 1 shows, this obscura-

tion by cold dust (which was not included in the Chakrabarti et al. (2008) simulations) is vital during the final burst to reprocess UV photons from young stars into FIR/submillimeter light.³

The predicted SEDs from SMGs formed by semi-analytic efforts show underluminous K -band and mid-IR fluxes by up to an order of magnitude. This may owe to SFRs and stellar masses in these SMGs which are roughly an order of magnitude lower than those inferred by observations (Baugh et al. 2005, 2007). While it is difficult to directly compare semi-analytic prescriptions with full N -body/SPH simulations, it is clear that varying treatments in the gas physics result in discrepant star formation histories, and consequent bulge masses and simulated SEDs. The plausible correspondence between the physical parameters and model SED from the models presented here and those observed owes to the detailed tracking of the starburst, star formation history, dust geometry and density distribution by these simulations. This suggests high resolution simulations are necessary to model the physical evolution of SMGs in detail.

That said, while the simulations presented in this work appear to provide a reasonable match to many observed parameters from SMGs, it is important to note that they, unlike the SAMs, *are not* cosmological in nature. For a galaxy formation model to be generic, it must concomitantly match the detailed physical and observable properties of a given population, as well as cosmological statistics. In this sense, the simulations presented here are complementary to the SAMs of SMG formation. The former reproduce detailed observables of SMGs in isolation via an *ab initio* model for SMG formation, though provide no information regarding cosmological statistics. The latter has some difficulty reproducing e.g. the observed SED, though accurately matches the observed number counts (as well as present day B, K and 60 μm -band luminosity functions; Baugh et al. 2005; Swinbank et al. 2008). The ideal scenario would be a coupling of the methods by convolving the lightcurves from high resolution hydrodynamic simulations of individual mergers to cosmological galaxy merger rates (e.g. Hopkins et al. 2009c) to investigate the statistical properties of SMGs. These efforts are currently underway.

³ Chakrabarti et al. (2008) incorporate a simplified, analytic model for the obscuring dust surrounding young stars. However, in contrast to our results, they find surprisingly little impact on the emergent IR SED, and even a moderate increase the rest-frame optical and near-UV luminosity.

ACKNOWLEDGMENTS

The authors thank Sukanya Chakrabarti, Laura Hainline, Dusan Keres and Mark Swinbank for helpful comments. We thank Laura Hainline for kindly providing Spitzer photometry of SMGs in advance of publication. The simulations in this paper were run on the Odyssey cluster supported by the Harvard FAS Research Computing Group. This project was funded in part by a grant from the W.M. Keck Foundation (TC), and by a Graduate Research Fellowship from the National Science Foundation (CH). JDY acknowledges support provided by NASA through Hubble Fellowship grant HF-51266.01 awarded by the Space Telescope Science Institute, which is operated by the Association of Universities for Research in Astronomy, Inc., for NASA, under contract NAS 5-26555. PJ was supported by programs HST-AR-10678 and 10958, provided by NASA through a grant from the Space Telescope Science Institute, which is operated by the Association of Universities for Research in Astronomy, Incorporated, under NASA contract NAS5-26555, and by Spitzer Theory Grant 30183 from the Jet Propulsion Laboratory.

References

- Alexander, D. M. et al. 2008, *AJ*, 135, 1968
 Baugh, C. M. et al. 2005, *MNRAS*, 356, 1191
 Baugh, C. M. et al. 2007, in *Astronomical Society of the Pacific Conference Series*, Vol. 375, *From Z-Machines to ALMA: (Sub)Millimeter Spectroscopy of Galaxies*, ed. A. J. Baker, J. Glenn, A. I. Harris, J. G. Mangum, & M. S. Yun, 7–
 Blain, A. W., Chapman, S. C., Smail, I., & Ivison, R. 2004, *ApJ*, 611, 725
 Blain, A. W. et al. 2002, *Phys. Rep.*, 369, 111
 Blitz, L. & Rosolowsky, E. 2006, *ApJ*, 650, 933
 Bondi, H. & Hoyle, F. 1944, *MNRAS*, 104, 273
 Borys, C., Smail, I., Chapman, S. C., Blain, A. W., Alexander, D. M., & Ivison, R. J. 2005, *ApJ*, 635, 853
 Bouché, N. et al. 2007, *ApJ*, 671, 303
 Chakrabarti, S., Fenner, Y., Cox, T. J., Hernquist, L., & Whitney, B. A. 2008, *ApJ*, 688, 972
 Chapman, S. C., Barger, A. J., Cowie, L. L., Scott, D., Borys, C., Capak, P., Fomalont, E. B., Lewis, G. F., Richards, E. A., Steffen, A. T., Wilson, G., & Yun, M. 2003a, *ApJ*, 585, 57
 Chapman, S. C., Blain, A. W., Ivison, R. J., & Smail, I. R. 2003b, *Nature*, 422, 695
 Chapman, S. C., Blain, A. W., Smail, I., & Ivison, R. J. 2005, *ApJ*, 622, 772
 Chapman, S. C. et al. 2004, *ApJ*, 611, 732
 Condon, J. J. 1992, *ARA&A*, 30, 575
 Coppin, K. et al. 2006, *MNRAS*, 372, 1621
 Cox, T. J. et al. 2006, *ApJ*, 650, 791
 Davé, R. 2008, *MNRAS*, 385, 147
 Davé, R., Hernquist, L., Katz, N., & Weinberg, D. H. 1999, *ApJ*, 511, 521
 Di Matteo, T., Springel, V., & Hernquist, L. 2005, *Nature*, 433, 604
 Downes, D. & Solomon, P. M. 1998, *ApJ*, 507, 615
 Draine, B. T. & Li, A. 2007, *ApJ*, 657, 810
 Dwek, E. 1998, *ApJ*, 501, 643
 Greve, T. R. et al. 2005, *MNRAS*, 359, 1165
 Groves, B., Dopita, M. A., Sutherland, R. S., Kewley, L. J., Fischera, J., Leitherer, C., Brandl, B., & van Breugel, W. 2008, *ApJS*, 176, 438
 Groves, B. A., Dopita, M. A., & Sutherland, R. S. 2004, *ApJS*, 153, 9
 Hernquist, L. 1990, *ApJ*, 356, 359
 Hopkins, P. F., Richards, G. T., & Hernquist, L. 2007, *ApJ*, 654, 731
 Hopkins, P. F. et al. 2005, *ApJ*, 625, L71
 —. 2006a, *ApJS*, 163, 1
 —. 2006b, *ApJS*, 163, 50
 —. 2008a, *ApJS*, 175, 356
 —. 2008b, *ApJS*, 175, 390
 —. 2008c, *ApJ*, 679, 156
 —. 2009a, *ApJS*, 181, 135
 —. 2009b, *ApJ*, 691, 1424
 —. 2009c, *ArXiv e-prints*
 Ivison, R. J., Greve, T. R., Smail, I., Dunlop, J. S., Roche, N. D., Scott, S. E., Page, M. J., Stevens, J. A., Almaini, O., Blain, A. W., Willott, C. J., Fox, M. J., Gilbank, D. G., Serjeant, S., & Hughes, D. H. 2002, *MNRAS*, 337, 1
 Jonsson, P. 2006, *MNRAS*, 372, 2
 Jonsson, P., Groves, B., & Cox, T. J. 2009, *ArXiv e-prints*
 Katz, N., Weinberg, D. H., & Hernquist, L. 1996, *ApJS*, 105, 19
 Kovács, A. et al. 2006, *ApJ*, 650, 592
 Leitherer, C. et al. 1999, *ApJS*, 123, 3
 Narayanan, D., Cox, T. J., Hayward, C., Younger, J. D., & Hernquist, L. 2009, *ArXiv e-prints: arXiv/0905.2184*
 Narayanan, D., Cox, T. J., Kelly, B., Davé, R., Hernquist, L., Di Matteo, T., Hopkins, P. F., Kulesa, C., Robertson, B., & Walker, C. K. 2008, *ApJS*, 176, 331
 Pope, A., Chary, R.-R., Alexander, D. M., Armus, L., Dickinson, M., Elbaz, D., Frayer, D., Scott, D., & Teplitz, H. 2008, *ApJ*, 675, 1171
 Pope, A. et al. 2006, *MNRAS*, 370, 1185
 Robertson, B., Hernquist, L., Cox, T. J., Di Matteo, T., Hopkins, P. F., Martini, P., & Springel, V. 2006, *ApJ*, 641, 90
 Sajina, A., Yan, L., Lutz, D., Steffen, A., Helou, G., Huynh, M., Frayer, D., Choi, P., Tacconi, L., & Dasyra, K. 2008, *ApJ*, 683, 659
 Sakamoto, K. et al. 1999, *ApJ*, 514, 68
 Sanders, D. B. & Mirabel, I. F. 1996, *ARA&A*, 34, 749
 Silva, L., Granato, G. L., Bressan, A., & Danese, L. 1998, *ApJ*, 509, 103
 Springel, V. 2005, *MNRAS*, 364, 1105
 Springel, V., Di Matteo, T., & Hernquist, L. 2005a, *ApJ*, 620, L79
 —. 2005b, *MNRAS*, 361, 776
 Springel, V. & Hernquist, L. 2002, *MNRAS*, 333, 649
 —. 2003, *MNRAS*, 339, 289
 Swinbank, A. M. et al. 2004, *ApJ*, 617, 64
 —. 2008, *MNRAS*, 391, 420
 Tacconi, L. J. et al. 2006, *ApJ*, 640, 228
 —. 2008, *ApJ*, 680, 246
 van Dokkum, P. G. 2008, *ApJ*, 674, 29
 Wagg, J., Owen, F., Bertoldi, F., Sawitzki, M., Carilli, C. L., Menten, K. M., & Voss, H. 2009, *ApJ*, 699, 1843
 Wilson, C. D. et al. 2008, *ApJS*, 178, 189
 Younger, J. D., Hayward, C. C., Narayanan, D., Cox, T. J., Hernquist, L., & Jonsson, P. 2009a, *MNRAS*, 396, L66
 Younger, J. D., Omont, A., Fiolet, N., Huang, J.-S., Fazio, G. G., Lai, K., Polletta, M., Rigopoulou, D., & Zylka, R. 2009b, *MNRAS*, 394, 1685
 Younger, J. D. et al. 2008a, *ApJ*, 688, 59
 —. 2008b, *ApJ*, 686, 815

